

Enhanced Dielectric Properties and Excellent Microwave Absorption of SiC Powders Driven with NiO Nanorings

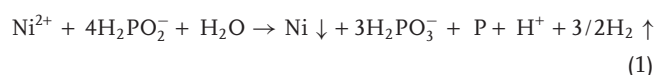
Huijing Yang, Maosheng Cao,* Yong Li, Honglong Shi, Zhiling Hou, Xiaoyong Fang, Haibo Jin,* Wenzhong Wang,* and Jie Yuan

Dielectric properties and weight are two key factors that can significantly influence the practical applications of electromagnetic (EM)-wave absorbing materials, which have been widely applied in civil, commercial, military, and aerospace vehicles in service in extreme environments.^[1–4] In addition, to use them in high temperatures, these materials should also have good thermal stability. Among many EM-wave absorbing materials, although silicon carbide (SiC) is has a good thermal stability,^[5–7] its dielectric properties are poor due to single polarization and low conductivity, limiting its practical applications greatly. Therefore, the development of multiple polarizations and improvement of the conductivity of SiC is very important to enhance its dielectric properties and thereby increase its practical applications.^[8] It has been reported that many methods can be employed to enhance dielectric properties of EM-wave absorbing materials.^[7,9] For instance, decorating composite materials with nanocrystals is an efficient route. On the basis of this route, we design a facile and novel strategy to improve the dielectric properties of SiC by assembling NiO nanorings on the surfaces of SiC powders, as shown in **Scheme 1a**. The NiO nanorings induce interfacial polarization between the nanocrystals and the substrate, and excite hopping charges, which lead to enhanced dielectric properties and excellent microwave absorption of the SiC powders.

NiO is a *p*-type semiconductor with a wide bandgap ranging from 3.6 to 4.0 eV,^[10] and has drawn much attention in potential applications of *p*-type transparent films,^[11] gas sensing devices,^[12,13] pollutant clean-up catalysts,^[9] dye-sensitized solar cells, and solid oxide fuel cells (SOFCs),^[14,15] due to its electronic, optical, and catalytic properties. Besides this, NiO is a kind of high-permittivity dielectric material, which has been intensively studied for use in important microelectronic devices such as capacitors and memory devices.^[16,17] Furthermore, NiO may significantly improve the dielectric properties of EM-wave absorbing materials owing to its high permittivity, oxidation resistance, and electronic properties.

In this work, we successfully cover ring-like NiO nanoparticles on the surfaces of SiC powders (NiO@SiC) by chemical deposition and oxidation. The dielectric properties of the fabricated NiO@SiC are systemically investigated in the temperature range from 373 to 773 K at frequencies of 8.2–12.4 GHz (X-band). The results show that the imaginary permittivity and loss tangent of NiO@SiC have been increased more than three times at 673 K compared to those of pure SiC. The reflection loss R_L peak of NiO@SiC can reach –46.9 dB at 673 K and is 330% lower than that of pure SiC, showing that NiO@SiC have excellent microwave absorption in the investigated temperature region.

Pure SiC powders are of irregular shape in the range from several hundreds nanometers to several micrometers. In order to improve the microwave absorption of SiC powders, we deposit ring-like NiO nanoparticles on the surfaces of SiC powders by the following two step process. Firstly, metal Ni nanoparticles are deposited on the surfaces of the powders. In this reaction process, a large amount of hydrogen gas bubbles is produced with the formation of Ni nanoparticles through the following reaction:^[18]



The formed hydrogen gas bubbles are attached to the surfaces of SiC by electrostatic interactions and can serve as soft templates for the formation of Ni nanorings, because the newly formed small Ni nanoparticles favor aggregation along the gas–liquid interface due to the minimization of interfacial energy. Thus, hollow Ni rings are formed on the surfaces of SiC powders. The formation process for Ni nanorings is similar to nanochains, nanotubes, hollow nanospheres, and honeycomb nanonets, as proposed in the literature.^[19] The formation mechanism for Ni nanorings is shown in **Scheme 1b**.

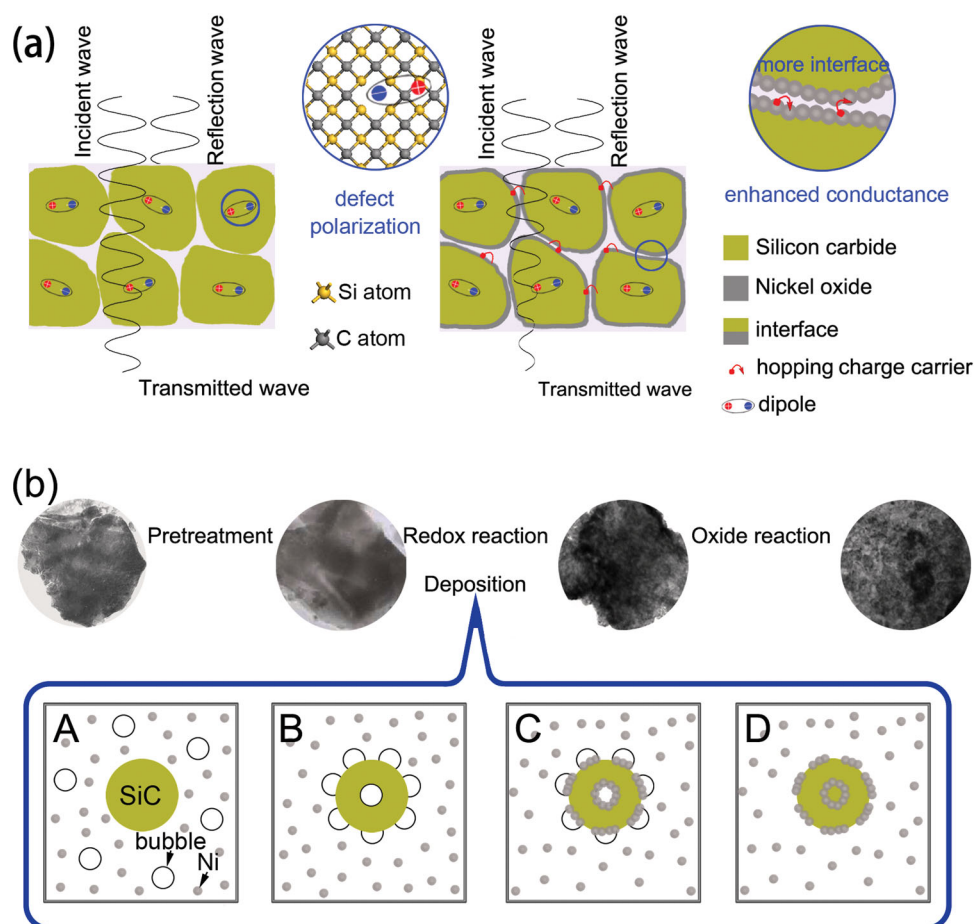
Secondly, the SiC powders loaded with Ni nanorings are heated at 923 K in air to convert Ni nanorings into NiO nanorings on the surfaces of SiC in situ, as illustrated in **Scheme 1b**.

Scanning electron microscope (SEM) images show that the SiC powders are uniformly covered by NiO nanoparticles, whose size is dozens of nanometers as shown in **Figure 1a–c**. From the transmission electron microscope (TEM) images (**Figure 1d–f**), it can be clearly seen that the surfaces of the SiC powders are covered uniformly with NiO nanoparticles, which exhibit ring-like morphology. The external diameter of the NiO nanorings is about 40–50 nm, and the internal diameter is approximately 25–35 nm. The corresponding high-resolution TEM (HRTEM) image of the NiO nanorings is presented in **Figure 1g**, showing that the nanorings are composed of nanocrystals with diameters of 5–10 nm, as marked

H. Yang, Prof. M. Cao, Y. Li, Z. Hou, X. Fang, H. Jin
School of Material Science and Engineering
Beijing Institute of Technology
Beijing, 100081, PR China
E-mail: caomaosheng@bit.edu.cn; hbjin@bit.edu.cn
H. Shi, Prof. W. Wang, J. Yuan
College of Science
Minzu University of China
Beijing, 100081, PR China
E-mail: wzhwangmuc@163.com



DOI: 10.1002/adom.201300439



Scheme 1. (a) Schematic approach to enhance the microwave absorption of SiC powders. (b) Schematic illustrations of the formation of Ni and NiO nanorings.

with red lines. It can also be found that the NiO nanocrystals in the nanorings compact firmly and have formed clear crystal boundaries. The clear lattice fringes and selected area electron diffraction (SAED) pattern illustrate that the NiO nanorings are composed of highly crystallized nanocrystals. The interplanar spacing is about 0.21 nm, corresponding to (200) planes of face-centered cubic NiO. The random SAED pattern is collected from a blend phase of NiO and SiC shown in Figure 1h, and then it is projected into a 1D diffraction profile (Figure 1i). The 1D diffraction profile is exported to a X-Y data file to identify phases using an X-ray diffraction (XRD) analysis package.^[20] The NiO phase is marked with pink bars, and SiC phase is shown with green bars. Results indicate that the specimen includes two phases: nickel oxide and silicon carbide.

The complex permittivity (including real and imaginary permittivities described as $\epsilon = \epsilon' - i\epsilon''$) of the samples is measured in the temperature range from 373 to 773 K at 8.2–12.4 GHz (X-band) to investigate the dielectric properties of NiO@SiC powders. **Figure 2** shows the plots of complex permittivity versus frequency for NiO@SiC samples and pure SiC samples at six different temperatures (303 K, 373 K, 473 K, 573 K, 673 K, and 773 K). The complex permittivity of NiO@SiC changes slightly from room temperature to 373 K. The results show that both real

and imaginary permittivities exhibit a decreasing trend with the increase of frequency, indicating the dielectric relaxation characteristic of the samples. More importantly, it can be noticed that the imaginary permittivity of NiO@SiC is almost four times higher than that of pure SiC at 773 K, while the real permittivity increases slightly, by nearly 15%. The loss tangent $\tan\delta_e$ (ratio of real permittivity to imaginary permittivity) can be calculated from the above experimental data. The results show that the loss tangent of NiO@SiC is almost 350% higher than that of pure SiC at 773 K.

Figure 3 shows the plots of complex permittivity versus temperature for NiO@SiC samples and pure SiC samples at four different frequencies (9 GHz, 10 GHz, 11 GHz, and 12 GHz). The imaginary permittivity of NiO@SiC samples dramatically increases more than four times, while the imaginary permittivity of pure SiC merely increases 15% from 373 to 773 K. One also can find that the real permittivity of NiO@SiC samples increases by almost double in the same temperature range. It can be estimated that the $\tan\delta_e$ increases from 0.21 to 0.59 with the temperature increasing from 373 to 773 K, and the maximum $\tan\delta_e$ of NiO@SiC is more than four times that of pure SiC. The results show that the permittivity of NiO@SiC exhibits strong temperature dependence. Additionally, the conductivity-temperature fitting curves

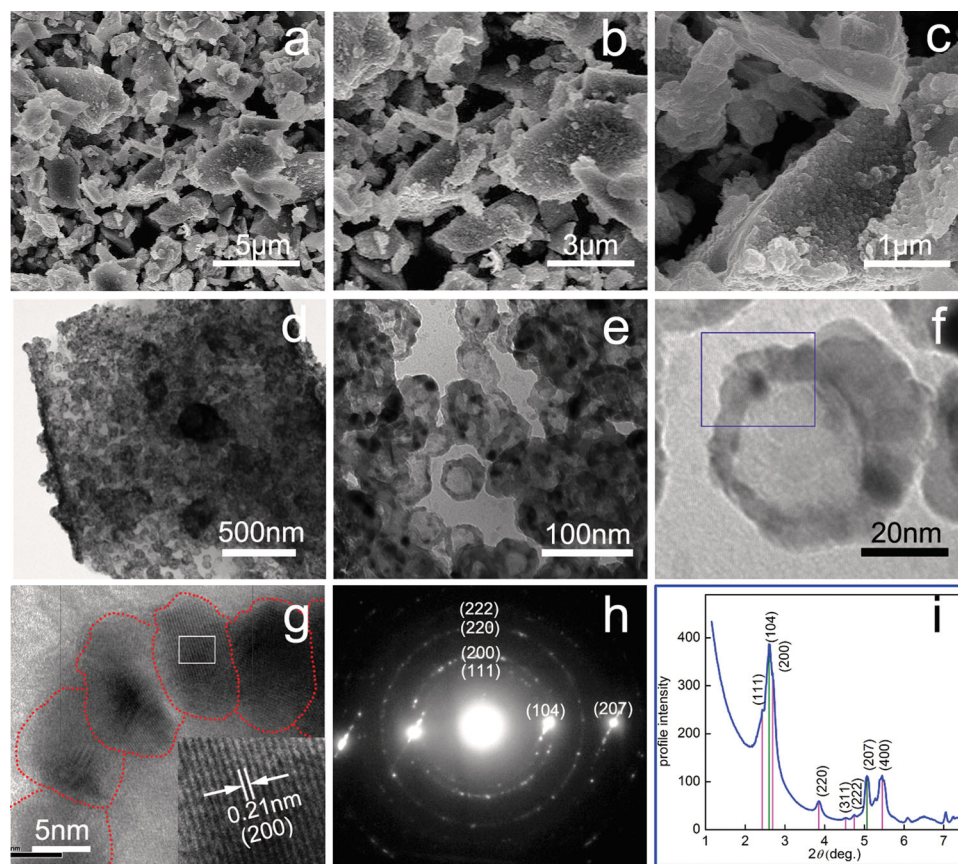


Figure 1. SEM images with different magnification of the NiO nanocrystals deposited on SiC powders (a–c). TEM images of NiO nanorings deposited on SiC powders (d–e). HRTEM image of a portion of one NiO nanoring (g). SAED pattern taken from NiO nanocrystals and SiC powders (h). 1D diffraction profile of the NiO and SiC generated by the rotation average of the SAED pattern (i), where NiO phase is marked as pink bars, and SiC phase is depicted as green bars.

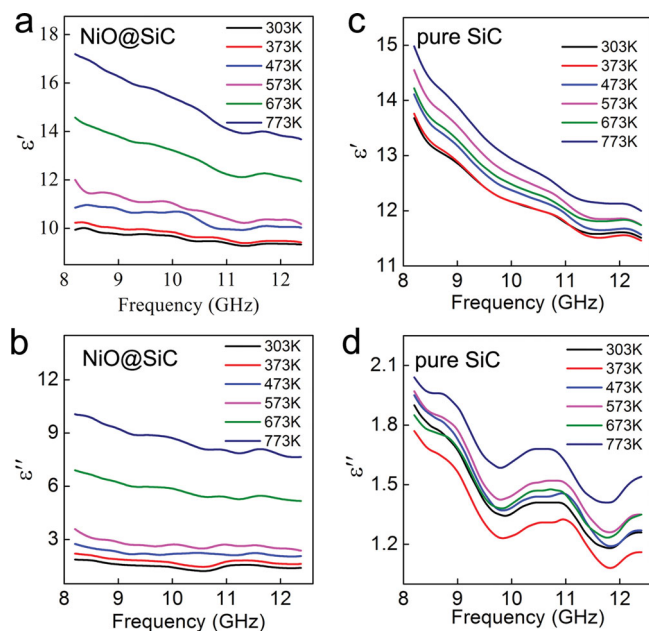


Figure 2. The plots of complex permittivity versus frequency of NiO@SiC (a,b) and pure SiC (c,d).

of the experimental data were obtained by the Debye Equation, which are shown in Figure 3c,f.^[21] It can be seen that the conductivity of NiO@SiC significantly increases with the increase of temperature, while the conductivity of pure SiC changes slightly. The relation between logarithm of conductivity and reciprocal of temperature is approximate linear for both NiO@SiC and pure SiC.

To further evaluate the microwave absorption of the SiC covered with NiO nanorings, we have systemically calculated the reflection loss R_L of NiO@SiC from the measured complex permittivity according to transmission line theory. The reflection loss R_L of EM wave (normal incidence) at the surface of a single-layer material backed by a perfect conductor at a given frequency and layer thickness can be defined as^[22]

$$R_L = 20 \log \left| \frac{Z_{in} - 1}{Z_{in} + 1} \right| \quad (2)$$

Here the normalized input impedance Z_{in} of microwave absorption layer can be expressed as

$$Z_{in} = \sqrt{\frac{\mu_r}{\epsilon_r}} \tanh \left[j \frac{2\pi}{c} \sqrt{\mu_r \epsilon_r} f d \right] \quad (3)$$

where c is the light velocity in vacuum, f is the microwave frequency, d is the thickness of the absorber, ϵ_r and μ_r are the

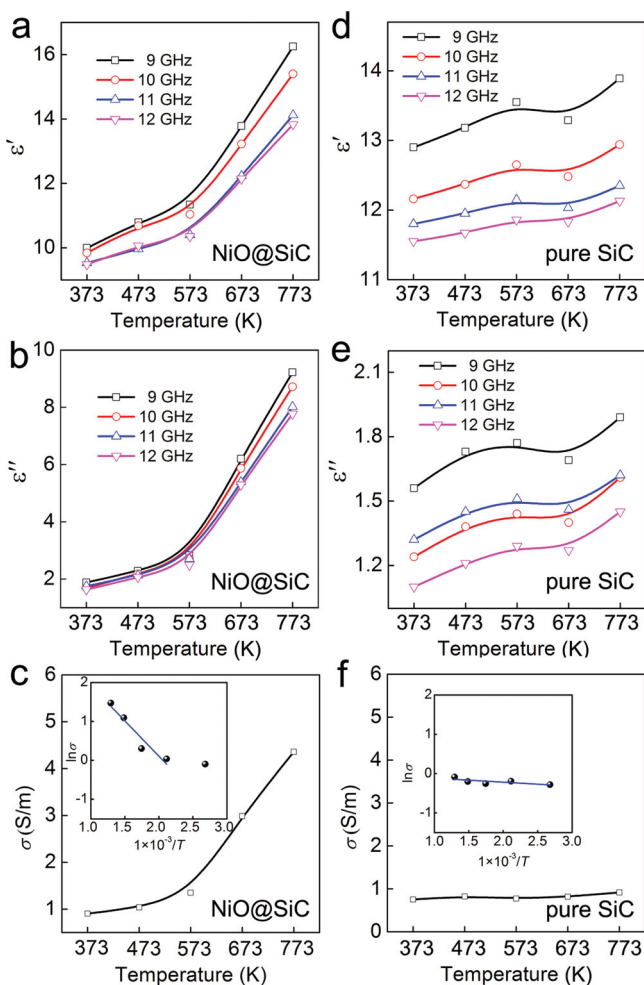


Figure 3. The plots of complex permittivity versus temperature of NiO@SiC (a,b) and pure SiC (d,e). The conductivity fitting curves of NiO@SiC (c) and pure SiC (f) based on the Debye Equation, the insets is the relation between logarithms of conductivity and reciprocal of temperature.

relative permittivity and permeability of the composite medium, respectively.

Figure 4a–d shows the 3D plots and contour plots of reflection loss R_L versus frequencies (F), temperatures (T) and thickness (d). From Figure 4a, it can be found that the minimum reflection loss R_L of NiO@SiC reaches -46.9 dB at 673 K and 10.6 GHz when the thickness is 2 mm. The R_L peaks firstly decrease from -18.1 dB at 12.4 GHz and 373 K to -46.9 dB at 10.6 GHz and 673 K, and then increase to -25.9 dB at 9.3 GHz and 773 K. The minimum absorbing peaks shift towards lower frequency (along the red arrow) with increasing temperatures as shown in Figure 4b. When the thickness of the EM wave absorbing materials is odd multiple of a quarter-wavelength, the reflection loss R_L can reach to an optimum value. This can be verified by our experimental results, in which the minimum value (-46.9 dB) of the reflection loss R_L is clearly observed when the thickness of the composite materials is quarter-wavelength (the black line $d = \lambda/4$) as presented in Figure 4d. Figure 4e,f show the 3D plots and contour plots of reflection loss R_L versus real and imaginary permittivities when the thickness is 2 mm at a frequency of 10.6 GHz. The

red dashed lines in Figure 4f show the R_L peaks of NiO@SiC at different temperatures while the conditions are kept constant. The blue point is the R_L peak of pure SiC. In Figure 4b,d,f, the contour lines of -10 dB and -20 dB are plotted by navy dashed lines. The above results indicate that the microwave absorption can be controlled by temperature, thickness, and permittivity.

Compared with the pure SiC, the as-fabricated NiO@SiC via our present strategy exhibits superior microwave absorption at the X-band, especially at high temperature, as shown in Figure 5. The R_L peak of NiO@SiC is more than three times than that of pure SiC at 673 K. The corresponding absorption bandwidths of pure SiC and NiO@SiC exhibit a widening tendency with the increase of temperatures when the reflection loss R_L is -10 dB. The absorption bandwidth of NiO@SiC is much wider than that of pure SiC at high temperature. In particular, the absorption bandwidths of NiO@SiC cover the whole X-band at temperatures of 673 and 773 K when the R_L reach to -10 dB. The results indicate that NiO@SiC powders is a promising candidate for EM-wave absorption material especially at high temperatures.

The excellent microwave absorption properties of NiO@SiC are attributed to the high loss tangent $\text{tg}\delta_e$ of NiO nanorings, which is determined by imaginary permittivity. According to the theory of EM fields, imaginary permittivity is generally determined by the orientational relaxation loss of intrinsic dipoles^[23] and electrical conductivity. From Figure 3b, it can be found that the polarization effect of dipoles becomes weak, while the conductivity increases with the increase of temperature. Hence, we can conclude that the loss tangent $\text{tg}\delta_e$ caused by conductance plays a key role in the imaginary permittivity. The enhanced electrical conductivity of NiO@SiC is mainly attributed to hopping charge carriers excited in the NiO nanorings due to oxygen vacancies introduced by incomplete oxidation. Oxygen vacancies may also improve the conductivity through inducing impurity states into the band structure of the NiO crystals, which can significantly narrow the bandgap of NiO.^[24] Under the EM field, the charge carriers hop between the adjacent NiO nanoparticles at high temperature, as shown in Scheme 1a. The conductivity is dominated by density and mobility of hopping charge carriers excited in the NiO nanorings. With the increase of temperature, the oxygen vacancies will reduce and the density may decline, however, the mobility is proportional to the function $\exp(-E/kT)$.^[25] As a result, the conductivity will increase with the temperature increase, as shown in Figure 3c. Due to the special ring-like structure of the NiO nanostructures, microcurrents induced by the EM wave can also increase the loss tangent $\text{tg}\delta_e$.^[26] Therefore, the imaginary permittivity and the loss tangent markedly increase with the increase of temperature, leading to the excellent microwave absorption properties of NiO@SiC.

In conclusion, we have fabricated NiO nanorings on the surfaces of SiC powders by a facile two-step strategy. The as-prepared NiO@SiC exhibits enhanced dielectric properties and excellent microwave absorption in the temperature range from 373 to 773 K due to the special ring-like morphology of the NiO nanocrystals. The loss tangent $\text{tg}\delta_e$ of NiO@SiC is almost 350% higher than that of pure SiC at 773 K. The minimum value of the reflection loss R_L is -46.9 dB at 673 K, which is more than three times that of pure SiC. Meanwhile, the absorption bandwidths of NiO@SiC cover the whole X-band at temperatures of 673 and 773 K when the reflection loss R_L is lower than -10 dB. The

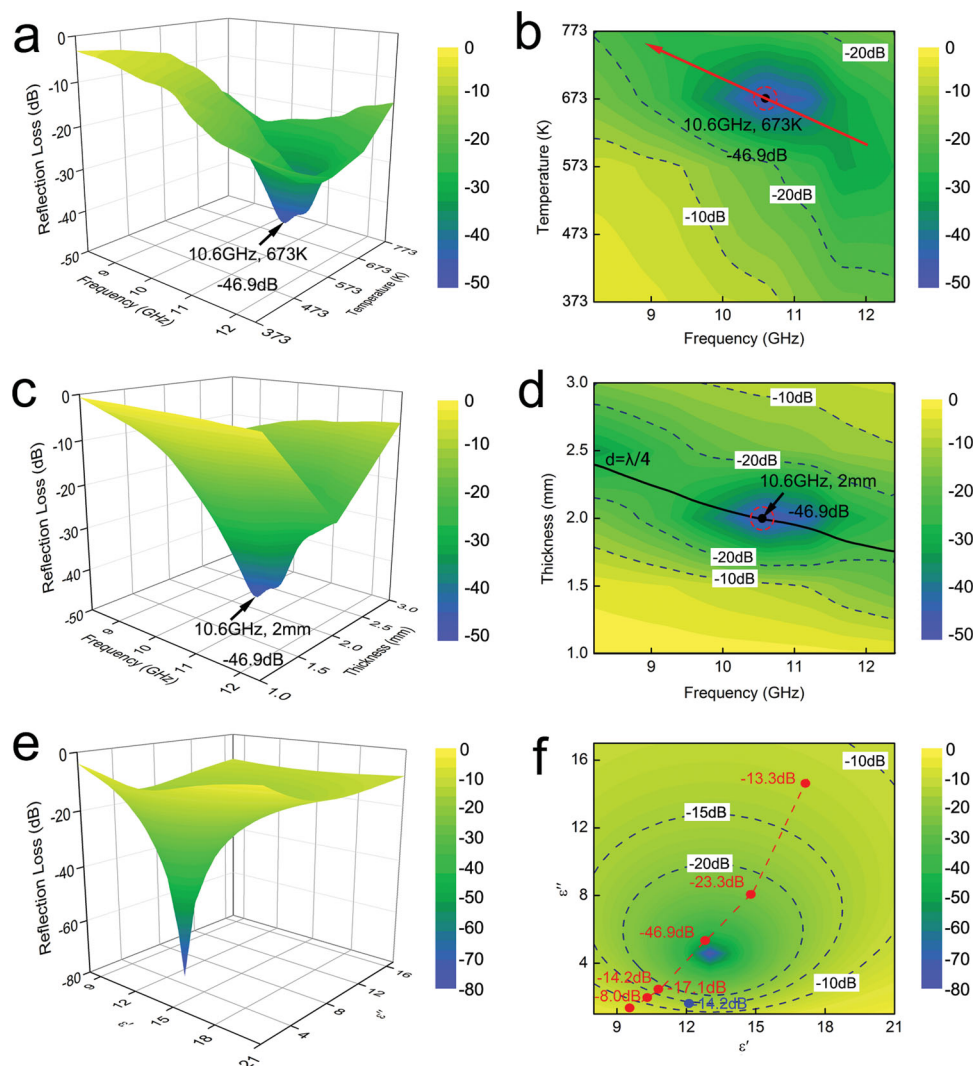


Figure 4. 3D plot and contour plot of the reflection loss versus frequency and temperature of NiO@SiC ($d = 2$ mm) (a,b). 3D plot and contour plot of the reflection loss versus frequency and thickness of NiO@SiC ($T = 673$ K) (c,d). 3D plot and contour plot of the reflection loss versus real permittivity and imaginary permittivity ($f = 10.5$ GHz and $d = 2$ mm) (e,f).

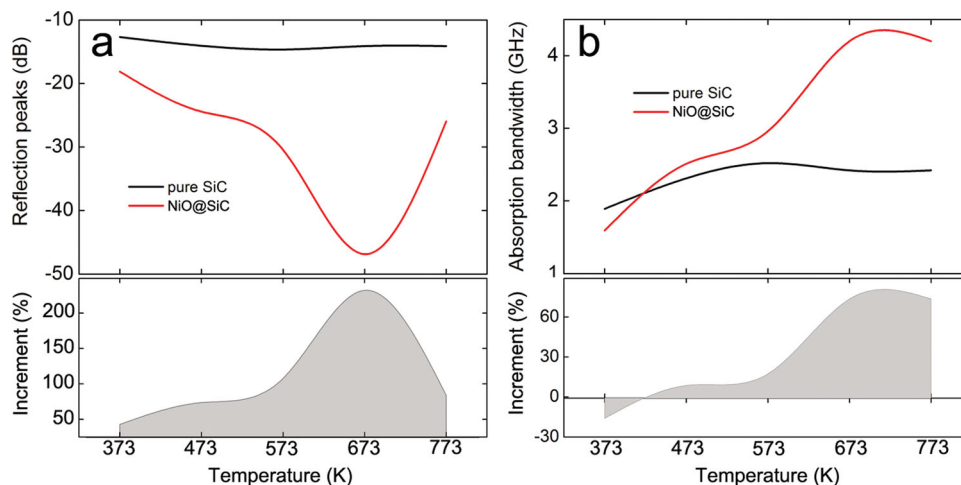


Figure 5. The plots of reflection loss peaks versus temperature and its increment compared NiO@SiC with pure SiC (a). The plots of absorption bandwidth ($R_L < -10$ dB) versus temperature and its increment compared NiO@SiC with pure SiC (b).

prepared NiO@SiC can be used as a considerable potential EM-wave absorption material with a light weight, thermal stability, strong microwave absorption, and wide bandwidth, especially at high temperature. Hence, the fabrication of this novel material provides a new approach to enhance the dielectric properties and microwave absorption of EM-wave absorbing materials.

Experimental Section

Materials: In the experiments, the SiC powders with particle sizes ranging from 500 nm to 5 μ m were commercially purchased from North Star Special Ceramics Co., Ltd.. Nickel chloride ($\text{NiCl}_2 \cdot 6\text{H}_2\text{O}$), nickel sulfate ($\text{NiSO}_4 \cdot 6\text{H}_2\text{O}$), sodium hypophosphite ($\text{NaH}_2\text{PO}_2 \cdot 2\text{H}_2\text{O}$), ammonium chloride (NH_4Cl), sodium citrate ($\text{Na}_2\text{C}_6\text{H}_5\text{O}_7 \cdot 2\text{H}_2\text{O}$), lead nitrate ($\text{Pb}(\text{NO}_3)_2$), stannous chloride (SnCl_2) and palladium chloride (PdCl_2) were purchased from Sinopharm Chemical Reagent Co., Ltd.. All chemicals used in this study were of analytical reagent grade and used as received without further purification.

Pretreatment of SiC Powders: The as-received SiC powders were first oxidized to remove organic impurities at 473 K in atmosphere for 2 h. After oxidation, SiC powders were introduced to a hydrophilic mixture solution of 10% HF and 10% HCl for 5 min and then ultrasonically dispersed for 20 min to improve the hydrophilic properties. Thirdly, the as-treated SiC powders were sensitized in a solution of 0.1 M SnCl_2 and 0.1 M HCl for 30 min. Finally, the powders were kept into a solution of 0.2 M PdCl_2 and 0.25 M HCl for 30 min to activate the powders.

Deposition of Ni Deposited on the Surfaces of SiC Powders by Replacement Deposition: After pre-treatments, SiC powders were dispersed in an alkaline solution (pH \sim 9.0) with a mixture of 0.25 M $\text{NiCl}_2 \cdot 6\text{H}_2\text{O}$, 0.09 M $\text{NiSO}_4 \cdot 6\text{H}_2\text{O}$, 0.13 M $\text{NaH}_2\text{PO}_2 \cdot 2\text{H}_2\text{O}$, 1.56 M NH_4Cl , 0.09 M $\text{Na}_2\text{C}_6\text{H}_5\text{O}_7 \cdot 2\text{H}_2\text{O}$ and 2.7×10^{-3} M $\text{Pb}(\text{NO}_3)_2$ at temperature of 318 K. The solution was stirred slowly to deposit uniformly. After 60 min, the mixture solution was filtered to collect treated-SiC powders, followed by washing with distilled water until pH neutral and then dried at 323 K.

Synthesis of SiC Powders Covered with NiO Nanorings by Oxidation: After deposition of Ni nanoparticles on the surfaces of SiC powders, the as-treated powders were heated at a rate 10 K/min to 923 K in air for 2 h and cooled to room temperature.

Characterization: The powders were characterized by transmission electron microscopy (TEM, JEOL-2100, Japan), scanning electron microscopy (SEM, HITACHI S-4800, Japan) for further characterization.

Measurement and Evaluation: In the dielectric measurement, the tested NiO@SiC and SiC samples with a rectangular dimension of 22.86 mm \times 10.16 mm \times 1.58 mm via a cold press under 20 MPa pressure were performed on a vector network analyzer (VNA) (Anritsu37269D, Japan) at X-band by the waveguide method. In the procedure, the tested samples were positioned vertically in the center of test chamber and heated by an inner heater at 20 K/min. A period of 25 min was required for the system to stabilize when each set-point temperature was achieved in order to ensure the accuracy of measurement. The measurement method is same as the procedure reported in the work by Cao and co-workers.^[25]

Acknowledgements

This research was supported by the National Science Foundation of P. R. China (Grant Nos. 51132002, 51372282, 50872159, 50972014 and 51072024).

Received: October 23, 2013

Revised: November 20, 2013

Published online: December 11, 2013

- [1] Z. M. Dang, T. Zhou, S. H. Yao, J. K. Yuan, J. W. Zha, H. T. Song, J. Y. Li, Q. Chen, W. T. Yang, J. Bai, *Adv. Mater.* **2009**, 21, 2077.
- [2] P. C. P. Watts, W. K. Hsu, A. Barnes, B. Chambers, *Adv. Mater.* **2003**, 15, 7.
- [3] Y. Duan, Z. Liu, H. Jing, Y. Zhang, S. Li, *J. Mater. Chem.* **2012**, 22, 18291.
- [4] Z. Chen, C. Xu, C. Ma, W. Ren, H. M. Cheng, *Adv. Mater.* **2013**, 25, 1296.
- [5] H. J. Yang, J. Yuan, Y. Li, Z. L. Hou, H. B. Jin, X. Y. Fang, M. S. Cao, *Solid State Commun.* **2013**, 163, 1.
- [6] J. G. Hartnett, D. Mouneyrac, J. Krupka, J. M. le Floch, M. E. Tobar, D. Cros, *J. Appl. Phys.* **2011**, 109, 064107.
- [7] D. Li, H. B. Jin, M. S. Cao, T. Chen, Y. K. Dou, B. Wen, *J. Am. Ceram. Soc.* **2011**, 94, 1523.
- [8] H. P. Xu, Z. M. Dang, M. J. Jiang, S. H. Yao, J. Bai, *J. Mater. Chem.* **2008**, 18, 229.
- [9] G. Zheng, X. Yin, S. Liu, X. Liu, J. Deng, Q. Li, *J. Eur. Ceram. Soc.* **2013**, 33, 2173.
- [10] X. Tong, Y. Qin, X. Guo, O. Moutanabbir, X. Ao, E. Pippel, L. Zhang, M. Knez, *Small* **2012**, 8, 3390.
- [11] B. L. Cushing, V. L. Kolesnichenko, C. J. O'Connor, *Chem. Rev.* **2004**, 104, 3893.
- [12] V. V. Plashnitsa, V. Gupta, N. Miura, *Electrochim. Acta* **2010**, 55, 6941.
- [13] G. Mattei, P. Mazzoldi, M. L. Post, D. Buso, M. Guglielmi, A. Martucci, *Adv. Mater.* **2007**, 19, 561.
- [14] M. D. Irwin, J. D. Servaites, D. B. Buchholz, B. J. Leever, J. Liu, J. D. Emery, M. Zhang, J. Song, M. F. Durstock, A. J. Freeman, M. J. Bedzyk, M. C. Hersam, R. P. H. Chang, M. A. Ratner, T. J. Marks, *Chem. Mater.* **2011**, 23, 2218.
- [15] P. Qin, M. Linder, T. Brinck, G. Boschloo, A. Hagfeldt, L. Sun, *Adv. Mater.* **2009**, 21, 2993.
- [16] K. Chen, S. K. Yuan, P. L. Li, F. Gao, J. Liu, G. L. Li, A. G. Zhao, X. M. Lu, J. M. Liu, J. S. Zhu, *J. Appl. Phys.* **2007**, 102, 034103.
- [17] Y. Lin, L. Jiang, R. Zhao, C. W. Nan, *Phys. Rev. B* **2005**, 72, 014103.
- [18] R. H. Guo, S. X. Jiang, Y. D. Zheng, J. W. Lan, *J. Appl. Polym. Sci.* **2012**, 127, 4186.
- [19] a) L. Guo, F. Liang, X. Wen, S. Yang, L. He, W. Zheng, C. Chen, Q. Zhong, *Adv. Funct. Mater.* **2007**, 17, 425; b) G. Tong, J. Guan, Q. Zhang, *Adv. Funct. Mater.* **2013**, 23, 2406; c) B. J. Plowman, A. P. O'Mullane, P. R. Selvakannan, S. K. Bhargava, *Chem. Commun.* **2010**, 46, 9182; d) Q. Liu, H. Liu, M. Han, J. Zhu, Y. Liang, Z. Xu, Y. Song, *Adv. Mater.* **2005**, 17, 1995.
- [20] H. Shi, G. Zhang, B. Zou, M. Luo, W. Wang, *Microsc. Res. Techniq.* **2013**, 76, 641.
- [21] B. Wen, M. Cao, Z. Hou, W. Song, L. Zhang, M. Lu, H. Jin, X. Fang, W. Wang, J. Yuan, *Carbon* **2013**, 65, 124.
- [22] a) J. Liu, R. Che, H. Chen, F. Zhang, F. Xia, Q. Wu, M. Wang, *Small* **2012**, 8, 1214; b) N. Tang, Y. Yang, K. Lin, W. Zhong, C. Au, Y. Du, *J. Phys. Chem. C* **2008**, 112, 10061.
- [23] Z. M. Dang, Y. Shen, L. Z. Fan, N. Cai, C. W. Nan, *J. Appl. Phys.* **2003**, 93, 5543.
- [24] B. Sasi, K. G. Gopchandran, P. K. Manoj, P. Koshy, P. Prabhakara Rao, V. K. Vaidyan, *Vacuum* **2002**, 68, 149.
- [25] M. S. Cao, W. L. Song, Z. L. Hou, B. Wen, J. Yuan, *Carbon* **2010**, 48, 788.
- [26] G. Wang, Z. Gao, S. Tang, C. Chen, F. Duan, S. Zhao, S. Lin, Y. Feng, L. Zhou, Y. Qin, *ACS Nano* **2012**, 6, 11009.